

Involvement of the Mitochondrion-dependent and the Endoplasmic Reticulum Stress-signaling Pathways in Isoliquiritigenin-induced Apoptosis of HeLa Cell*

YUAN Xuan¹, ZHANG Bo³, GAN Lu⁴, WANG Zhen Hua⁴, YU Ba Cui³,
LIU Liang Liang³, ZHENG Qiu Sheng^{2,#}, and WANG Zhi Ping^{1,#}

1. Lanzhou University Second Hospital, Lanzhou University, Lanzhou 730000, Gansu, China; 2. Life Science School, Yantai University, Yantai 264000, Shandong, China; 3. Key Laboratory of Xinjiang Endemic Phytomedicine Resources, Ministry of Education, School of Pharmacy, Shihezi University, Shihezi 832002, Xinjiang, China; 4. Institute of Modern Physics, Chinese Academy of Sciences, Lanzhou 730000, Gansu, China

Abstract

Objective Isoliquiritigenin (ISL), a licorice chalconoid, is considered to be a bioactive agent with chemopreventive potential. This study investigates the mechanisms involved in ISL-induced apoptosis in human cervical carcinoma HeLa cells.

Methods Cell viability was evaluated using a 3-(4, 5-dimethylthiazol-2-yl)-2, 5-diphenyl-tetrazolium bromide (MTT) assay. Apoptosis was determined by flow cytometry using an Annexin V-FITC Apoptosis Detection Kit. The intracellular ROS levels were assessed using a 2, 7-dichlorofluorescein probe assay. The mitochondrial membrane potential was measured with the dual-emission potential-sensitive probe 5, 5', 6, 6'-tetra-chloro-1, 1', 3, 3'-tetraethyl-imidacarbocyanine iodide (JC-1). The degradation of poly-ADP-ribose polymerase (PARP) protein, the phosphorylation of PKR-like ER kinase (PERK), the phosphorylation of the α -subunit of eukaryotic initiation factor 2 (eIF2 α), the expression of the 78 kD glucose-regulated protein (GRP 78), and the activation of caspase-12 were analyzed via western blot analysis.

Results ISL significantly inhibited the proliferation, the increase in ROS levels and apoptotic rates of HeLa cells in a concentration-dependent manner. Moreover, ISL induced mitochondrial dysfunction, caspase activation, and PARP cleavage, which displayed features of mitochondria dependent on apoptotic signals. Besides, exposure of HeLa cells to ISL triggered endoplasmic reticulum (ER) stress, as indicated by the increase in p-eIF2 α and GRP78 expression, ER stress-dependent apoptosis is caused by the activation of ER-specific caspase-12.

Conclusion The findings from our study suggest that ISL-induced oxidative stress causes HeLa cell apoptosis via the mitochondrion-dependent and the ER stress-triggered signaling pathways.

Key words: ISL; HeLa cells; ROS; Mitochondria; ER stress; Apoptosis

Biomed Environ Sci, 2013; 26(4):268-276 doi: 10.3967/0895-3988.2013.04.005 ISSN:0895-3988

www.besjournal.com/full_text

CN: 11-2816/Q

Copyright ©2013 by China CDC

*This study was supported by the National Natural Science Foundation of China (No. 30960451), Major State Basic Research Development Program (2010CB535003), and the Xinjiang production and construction corps funds for distinguished young scientists to ZHENG Qiu Sheng, international cooperation projects (2012BC001).

#Correspondence should be addressed to WANG Zhi Ping, Tel: 86-0931-8912106, Fax: 86-0931-8942821, E-mail: erywzp@lzu.edu.cn; ZHENG Qiu Sheng, Tel: 86-0993-2057003, Fax: 86-0993-2057005, E-mail: zqsy@sohu.com

Biographical note of the first author: YUAN Xuan, female, born in 1982, Ph. D candidate, majoring in tumor molecular biological.

INTRODUCTION

Licoriritigenin (ISL) is existing in licorice and vegetables such as shallots and bean sprouts^[1-2]. ISL has shown a variety of biological activities including antioxidant^[3-4], anti-inflammatory^[5], estrogenic^[6], chemopreventive^[7-8], and anti-tumor properties^[9]. ISL reportedly inhibits cell growth and induces apoptosis in lung^[10], gastric^[11], hepatic^[12], prostatic^[13-14], colon^[15-17], and skin cancer cells^[18]. These studies strongly support the use of ISL in chemoprevention of human cancer.

The endoplasmic reticulum (ER), a major intracellular organelle, is a quality control system for intracellular protein homeostasis and it controls the synthesis, folding, and delivery of biologically active proteins^[19-20]. The accumulation of unfolded or misfolded proteins in the ER lumen, which induces a coordinated adaptive program, are called the unfolded protein response (UPR), causing ER stress^[21]. Increasing evidence show that ER stress plays a critical role in the apoptosis regulation caused by oxidative stress^[22-23]. On the other hand, the production of reactive oxygen species (ROS) is induced by misfolded ER proteins, which activate the UPR and contribute to the induction of apoptosis^[24-25].

ROS are formed as byproducts of the normal cellular metabolism of oxygen^[26]. Organisms have developed antioxidant systems that include antioxidant enzymes, such as superoxide dismutase (SOD), and antioxidant molecules, such as glutathione (GSH), to balance these harmful radicals^[27]. However, oxidative stress, a condition characterized by a dramatic increase in ROS levels and disruption of antioxidant balance, results in oxidative damage to cellular structures, signal transduction, and cell death^[28]. In addition, ROS damages both DNA and proteins. Then, chemopreventive agents induce apoptosis in cancer cells through ROS generation^[29-31].

Several lines of evidence indicate that ISL has diverse pharmacological effects such as antioxidant^[3-4], anti-inflammatory^[5], and anti-tumor^[9,32-33]. However, few studies have shown that ISL induces apoptosis via oxidative stress, disrupting cellular functions and eventually causing apoptosis in HeLa. Therefore, this study is aimed to explore the role of ROS and the possible mechanisms of ISL-induced apoptosis in HeLa cells.

MATERIALS AND METHODS

Chemicals

ISL was purchased from Jiangxi Herb Tian gong Technology Co., Ltd. (Jiangxi, China). Dulbecco's modified Eagle's medium (DMEM), dimethylsulfoxide (DMSO) and acridine orange/ethidium bromide (AO/EB), N-acetylcysteine (NAC), a precursor of glutathione, provide important protection against ROS, and Annexin V/PI apoptosis kit, molecular Probes 2',7'-dichlorodihydrofluorescein diacetate (H₂DCFDA) were purchased from Sigma (St. Louis, Missouri, USA). Fetal bovine serum (FBS) was purchased from Tianjin Hao Yang Biological Manufacture Co., Ltd. (Tianjin, China). The antibodies used in this study were purchased from Santa Cruz Biotechnology Inc. (Santa Cruz, CA, USA). Penicillin and streptomycin were obtained from Shandong Sunrise Pharmaceutical Co., Ltd. (Shandong, China). ISL was dissolved in DMSO and diluted with fresh medium to achieve the desired concentration. The final concentration of DMSO did not exceed 0.2% in the fresh medium, and DMSO at this concentration had no significant effect on the cell viability. Unless indicated otherwise, the other reagents were purchased from Sigma.

Cell Culture

HeLa cells were purchased from China Center for Type Culture Collection (Wuhan, China). The cells were maintained in DMEM supplemented with 10% FBS, 100 U/mL penicillin and 100 µg/mL streptomycin at 37 °C with 5% CO₂. The cells were split every 3 days and were diluted every day before each experiment.

Cell Viability Assay

Cell viability was measured by the MTT [3-(4,5-dimethylthiazol-2-yl)-2,5-diphenyl-tetrazolium bromide] assay^[34]. In brief, cells were washed with fresh media and cultured in 96-well plates (1×10⁵ cells/mL) and then incubated with ISL (0, 2, 5, 10, 30, 40, 60 µg/mL) for 24 h. After incubation, the medium was aspirated and fresh medium containing 10 µL of 5 mg/mL MTT was added. After 4 h, the medium was removed and replaced with blue formazan crystal dissolved in 100 µL dimethyl sulfoxide (DMSO). Absorbance at 570 nm was measured using a fluorescent plate reader (Millipore Corp., Bedford, MA). The data were expressed as percent cell viability compared with control (DMSO).

Morphological Assay (AO/EB)

In order to explore whether ISL induces apoptosis in HeLa cells, the cells were plated on a four-well chamber slides at 20 000 cells/slide, and treated with increasing concentrations of ISL for 24 h to examine whether ISL induces apoptosis in HeLa cells. The cells were stained by 4 μ L of prepared acridine orange/ethidium bromide (AO/EB) working solution (100 mg/L AO and 100 mg/L EB in phosphate buffered saline) for 30 min in the dark at 37 °C. The cells in the slides were then inspected using fluorescence microscope^[35].

Detection of Intracellular Reactive Oxygen Species (ROS) Lever

ROS generated in HeLa cells was assessed using 2',7'-dichlorodihydrofluorescein diacetate (H₂DCFDA) probe^[36]. H₂DCFDA was deacetylated intracellularly by using a nonspecific esterase, which was further oxidized by cellular peroxides, yielding 2,7-dichlorofluorescein (DCF), a fluorescent compound ($\lambda_{EX}/\lambda_{EM}$ =485 nm/535 nm). Briefly, the cells were incubated with the indicated concentrations of ISL with or without NAC (200 μ mol/L) for 2 h. Cells were then washed in phosphate buffered saline (PBS) and incubated with 30 μ mol/L H₂DCFDA at 37 °C for 30 min, as indicated in the instructions of the manufacturer. DCF was detected by using a FACStar flow cytometer (Becton Dickinson, New Jersey, USA). Each group was acquired more than 10 000 individual cells.

Measurement of Malondialdehyde (MDA) Content

The formation of MDA, a substance produced during lipid peroxidation, was determined by the thiobarbituric acid reactive substances (TBARS) test^[37]. Briefly, after exposure to ISL alone or in combination with NAC for 24 h, HeLa cells were harvested and aliquots of 10% supernatant were incubated with 0.8% TBA. The mixture was heated in 95 °C water bath for 1 h. Afterwards, n-butanol and pyridine (15:1, V/V) were added and the mixture was centrifuged. The organic phase was collected to measure fluorescence at excitation and emission wavelengths of 515 and 553 nm respectively. A standard curve was generated by using 1, 1, 3, 3-tetramethoxypropane. MDA content was expressed as nmol/mg protein. Protein content was measured by the method of Bradford^[38] (1976).

Detection of Cell Apoptotic Rates by Flow Cytometry

Apoptosis was determined by staining cells

with annexin V fluorescein isothiocyanate (FITC) and propidium iodide (PI) labeling^[39]. Briefly, 1.5 \times 10⁵ cells/mL were incubated with ISL with or without NAC (200 μ mol/L) for 24 h. Afterwards, the cells were washed twice with ice-cold PBS, and then 5 μ L of annexin V-FITC (PharMingen, San Diego, CA) and 5 μ L of PI (1 mg/mL) were then applied to stain cells. The status of cell staining was analyzed by using the FACStar flow cytometer (Becton Dickinson). Viable cells were negative for both PI and annexin V-FITC; apoptotic cells were positive for annexin V-FITC and negative for PI, whereas late apoptotic dead cells displayed strong annexin V-FITC and PI labeling. Non-viable cells, which underwent necrosis, were positive for PI but negative for annexin V-FITC.

Measurement of Mitochondrial Membrane Potential

In order to measure the mitochondrial membrane potential, the dual-emission potential-sensitive probe 5, 5', 6, 6'-tetra-chloro-1, 1', 3, 3'-tetraethyl-imidacarbocyanine iodide (JC-1) was used. JC-1 is a green-fluorescent monomer at low membrane potential, with the membrane potential of energized mitochondria promoting the formation of red-fluorescent J-aggregates. The ratio of red to green fluorescence of JC-1 depends only on the membrane potential, with a decrease being indicative of membrane depolarization^[40-41]. HeLa cells treated with ISL were harvested in the absence or presence of NAC (200 μ mol/L). Then, the cells were loaded with 2 mg/L of JC-1 at 37 °C for 20 min and analyzed afterwards by using a plate reader (Millipore Corp., Bedford, MA, USA).

Measurement of Caspase Activities

The activities of caspase-3 and caspase-9 were assessed by using the caspase-3 and caspase-9 Colorimetric Assay Kits (R&D systems, Inc., Minneapolis, USA), which are based on the spectrophotometric detection of the color reporter molecule p-nitroaniline (pNA) after cleavage from the labeled substrate DEVD-pNA (caspase-3) and LEHD-pNA (caspase-9) as an index respectively. In brief, cells were incubated with the designated concentration of ISL in the absence or presence of NAC (200 μ mol/L). The cells were then washed by PBS and suspended in 5 volumes of lysis buffer (20 mmol/L Hepes, pH 7.9, 20% Glycerol, 200 mmol/L KCl, 0.5 mmol/L EDTA, 0.5% NP40, 0.5 mmol/L DTT, 1% protease inhibitor cocktail (from Sigma). The lysates were then collected and stored at -20 °C until

use. Protein concentration was determined by the Bradford method. Supernatant samples, containing 100 µg of total protein, were added to 96-well plates (Nunc, Roskilde, Denmark) with the DEVD-pNA and LEHD-pNA at 37 °C for 1-2 h to determine caspase-3 and caspase-9 activities. The optical density of each well was measured at 405 nm by using the microplate reader (Millipore Corp., Bedford, MA). Each plate contained the multiple wells of a given experimental condition and multiple control wells. The activities of caspase-3 and caspase-9 were expressed in arbitrary absorbance units (absorbance at a wavelength of 405 nm/L).

Western Blot Analysis and Statistical Analysis

The soluble lysates (15 µL per lane) were subjected to 10% sodium dodecyl sulfate-polyacrylamide gel electrophoresis (SDS-PAGE), and then transferred onto the nitrocellulose membranes (Amersham Biosciences, New Jersey, USA) and blocked with 5% nonfat milk in Tris-buffered saline with Tween (TBST) for 2 h at room temperature. Membranes were incubated with anti-glucose-regulated protein, 78/immunoglobulin heavy chain-binding protein (78 kD glucose-regulated protein, GRP78) antibody (1:200), anti-poly-ADP-ribose polymerase (PARP) antibody (1:500), anti-caspase-12 antibody (1:200), anti-phosphorylation of α -subunit of eukaryotic initiation factor 2 (eIF2 α) antibody (1:200), anti-phosphorylation of PKR-like ER kinase (PERK) antibody, anti- β -actin antibody (1:2000) (Santa Cruz Biotechnology, Santa Cruz, CA, USA) in 5% milk/TBST at 4 °C overnight. After washing membranes with TBST five times, the membranes were incubated with horseradish peroxidase-conjugated antibody for 1 h at room temperature. Western blots were developed by using enhanced chemiluminescence (ECL, thermo) and were exposed on Kodak radiographic film.

The data were presented as means \pm S.E. from at least three independent experiments and evaluated through the analysis of variance (ANOVA) followed by student's *t* test. The values of $P < 0.05$ were considered statistically significant. The analyses were performed by using the Origin 6.0 software (Origin Lab Corporation, Northampton, MA, USA)

RESULTS

Effects of ISL on Cell Viability and ROS Production in HeLa Cells

HeLa cells were cultured for 24 h with different ISL concentrations (0, 2, 5, 10, 30, 40, and 60 µg/mL)

in order to examine its effects on HeLa cell viability. Cell viability was measured using an MTT assay. A significant concentration-dependent reduction in cell viability was observed, and cell inhibition rates ranged from 25% to 76% after 24 h of ISL treatment (Figure 1). After the HeLa cells were exposure to ISL (10, 30, and 60 µg/mL) for 2 h, the intracellular ROS (using DCF fluorescence as an indicator for ROS formation) and MDA (an index of oxidative damage to membrane lipids) levels were significantly increased in a concentration-dependent manner compared with the control group (Figure 2). The antioxidant *N*-acetylcysteine (NAC, a precursor of glutathione, 200 µmol/L) effectively prevented ISL-induced ROS formation and MDA levels (Figure 2).

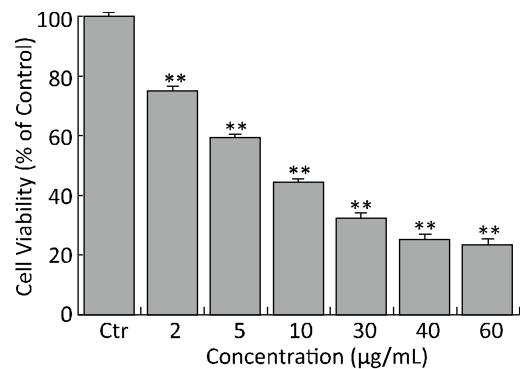


Figure 1. Effects of ISL on cell viability of HeLa cells. Cell viability was determined by using an MTT staining assay. Treatment of HeLa cells with varying ISL concentrations (0, 2, 5, 10, 30, 40, and 60 µg/mL) for 24 h resulted in a significant concentration-dependent reduction in cell viability. The data represent the means \pm S.E. of the three independent experiments. ** $P < 0.01$ compared with the ISL-untreated control group cells.

ISL-induced Apoptosis Is Mediated by a Mitochondrion-dependent Pathway in HeLa Cells

Morphologic measurement results obtained by using AO/EB staining (Figure 3A) showed that normal viable HeLa cells were stained green (Ctr), and the apoptotic HeLa cells (10, 30, and 60 µg/mL) appeared as bright green arcs in its earliest stage and with condensed, yellow/orange nuclei in its late stage. Annexin V-FITC-PI double-staining was used to detect phosphatidyl serine (PS) externalization, a hallmark of early apoptosis, to prove whether ISL-induced apoptosis occurs. As shown in Figure 3B,

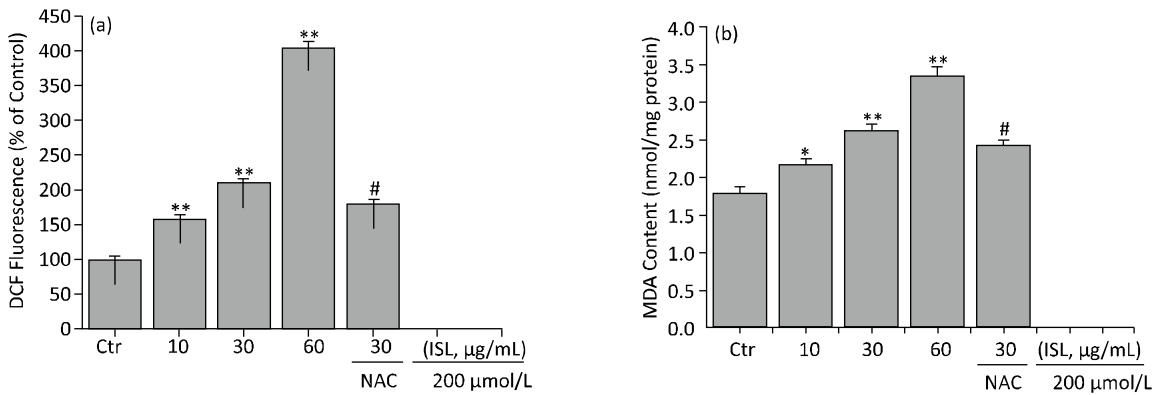


Figure 2. Effects of ISL on ROS and MDA production in HeLa cells. The cells were treated with ISL (0, 10, 30, and 60 µg/mL) with or without NAC (200 µmol/L). (a) ROS was determined via flow cytometry; (b) oxidative damage to membrane lipids (lipid peroxidation) was measured by using the levels of MDA. Data are presented as the mean±S.E. of the three independent experiments. * $P<0.05$, ** $P<0.01$ compared with the control group; # $P<0.05$ compared with the ISL group alone (30 µg/mL).

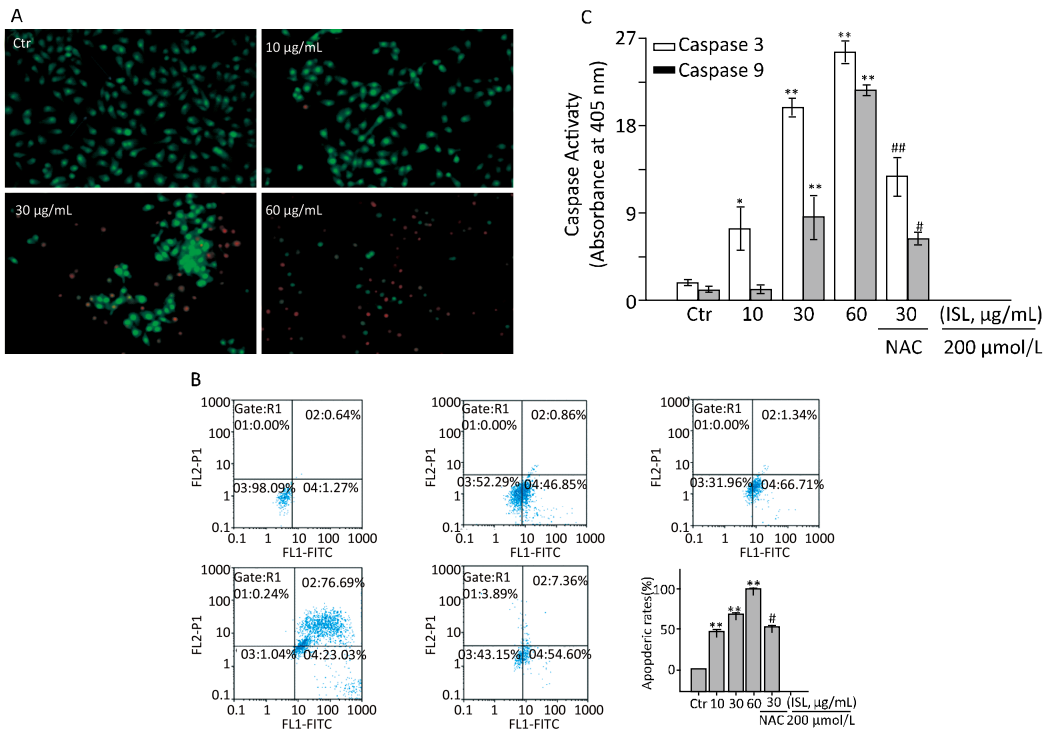


Figure 3. ISL induced apoptosis in HeLa cells. The cells were treated with or without the indicated amounts of ISL for 24 h with or without NAC (200 µmol/L). (A) Morphologic measurements in HeLa cells were carried out via AO/EB fluorescence staining. (B) Detection of apoptotic rates conducted via flow cytometry. (C) Caspase-3 and caspase-9 activity were examined. The data in C and D were presented as the mean±S.E. of the three independent experiments. * $P<0.05$, ** $P<0.01$ compared with the control group; # $P<0.05$, ## $P<0.01$ compared with the ISL group alone (30 µg/mL).

the apoptotic rates were markedly increased among ISL-treated cells, which indicates that these cells were in early apoptosis. In order to evaluate the apoptotic signaling induced by ISL, caspase-9 and

caspase-3 activity were measured. Caspase-9 is involved in the activation of the caspase cascade responsible for apoptosis induction, which then cleaves and activates caspase-3. Caspase-3 activity is

an integral step in most apoptotic events. In this study, treatment with ISL (10, 30, and 60 $\mu\text{g}/\text{mL}$) induced remarkable caspase-9 and caspase-3 activation (Figure 3C). Pretreatment with NAC (200 $\mu\text{mol}/\text{L}$) effectively prevented ISL-induced HeLa cell apoptosis (Figure 3). These results suggest that ISL-induced apoptosis may be associated with ROS production. In order to determine whether ISL-induced apoptosis is mediated through mitochondrial dysfunction, the mitochondrial membrane potential (MMP) is measured by using the mitochondrion-sensitive dye JC-1. As shown in Figures 4A, JC-1 accumulated in the untreated control cells, where it displayed bright red fluorescence, which indicates a high potential. By contrast, JC-1 poorly accumulated in ISL-treated cells, which displayed green fluorescence, thereby indicating disruption of the MMP. This result was further confirmed by calculating the mean red/green fluorescence ratio using a plate reader, which showed a concentration-dependent decrease in MMP after ISL treatment (Figure 4B). Meanwhile, as shown in Figure 4C, the levels of the 89 kD cleaved PARP fragment (the active form) was significantly increased after the HeLa cells were exposed to ISL for 24 h. These ISL-induced responses were alleviated by 200 $\mu\text{mol}/\text{L}$ NAC (Figure 4).

ISL Induces the Endoplasmic Reticulum (ER) Stress Response in HeLa Cells

The involvement of ER stress signaling in the responses triggered by ISL-induced apoptosis was evaluated based on the phosphorylation patterns of PKR-like ER kinase (PERK) and α -subunit of eukaryotic initiation factor 2 (eIF2 α). PERK, an ER-resident transmembrane kinase, is known to auto-phosphorylate its cytoplasmic kinase domain in response to the accumulation of unfolded proteins in the ER lumen. Activated PERK subsequently phosphorylates several cytosolic proteins such as eIF2 α . As shown in Figure 5, ISL increased the levels of p-PERK, p-eIF2 α , and GRP78, and the cleavage of caspase-12 with in 24 h of exposure. These effects were reversed by 200 $\mu\text{mol}/\text{L}$ NAC (Figure 5).

DISCUSSION

With the multistep development of human tumors, cancer cells acquire biological capabilities such as sustained proliferative signaling, evasion of growth suppressors, cell death resistance, replicative immortality, induction of angiogenesis, activation of

invasion and metastasis, reprogramming of energy metabolism, and evasion of immune destruction, which constitute an organizing principle for rationalizing the

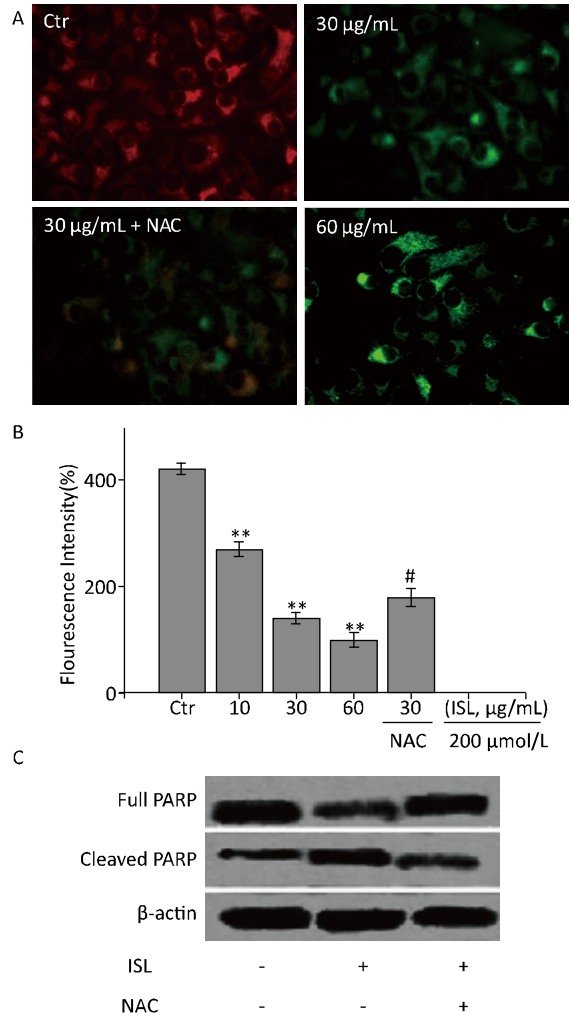


Figure 4. ISL induced mitochondrial dysfunction, cleavage of poly (ADP-ribose) polymerase (PARP), and caspase cascade activation in HeLa cells. The cells were treated with or without ISL (0, 10, 30, and 60 $\mu\text{g}/\text{mL}$) with or without NAC (200 $\mu\text{mol}/\text{L}$). (A) JC-1 fluorescence was monitored by using fluorescence microscopy. (B) Mitochondrial membrane potential depolarization was determined by using a fluorescence plate reader. (C) PARP cleavage was examined via western blot analysis. The data in B is presented as the mean \pm S.E. of three independent experiments. ** P <0.01 compared with the control group; # P <0.05 compared with the ISL group alone (30 $\mu\text{g}/\text{mL}$). The results shown in B are representative of at least three independent experiments.

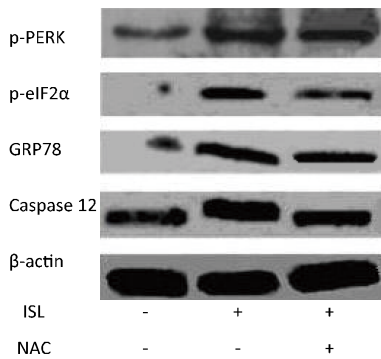


Figure 5. Effects of ISL on ER stress marker expression in HeLa cells. The cells were treated with or without ISL (30 $\mu\text{g}/\text{mL}$) with or without 200 $\mu\text{mol}/\text{L}$ NAC. The expression of p-PERK, p-eIF2 α , GRP78, and caspase-12 were analyzed via western blot analysis.

complexities of neoplastic disease. In addition to cancer cells, tumors exhibit another dimension of complexity. They contain a repertoire of recruited, ostensibly normal cells that contribute to the acquisition of hallmark traits by creating the 'tumor microenvironment.' Recognition of the widespread applicability will increasingly affect the development of new means to treating human cancer^[42].

Emerging evidence demonstrates that the anticancer activities of certain chemotherapeutic agents are involved in the induction of apoptosis, which is regarded as the preferred method for managing cancer^[43-44]. Several studies have shown that ISL is a potent anti-tumor-promoting agent, which educes cancer chemopreventive activity by inducing the apoptosis of cancer cell^[11,18]. However, the precise mechanisms underlying the apoptotic cell death caused by ISL are mostly unclear. The most important finding of this study is that ISL induces ROS generation, mitochondrial dysfunction, apoptotic cascade activation, and ER stress in HeLa cells. Moreover, these ISL-induced cytotoxic responses are alleviated by cotreatment with the antioxidant NAC. Therefore, these findings indicate that oxidative stress mediated mitochondrion-dependent and ER stress-activated apoptotic signals involved in ISL-induced HeLa cell apoptosis.

Mitochondrial dysfunction has been demonstrated to play a crucial role in cell apoptosis. Mitochondria are very sensitive to oxidative stress, and excess ROS causes perturbations in mitochondrial function, and subsequently triggers apoptosis^[45-46]. Killing tumor cells via cytotoxic therapy, for example, chemotherapy, γ -irradiation,

immunotherapy, or suicide gene therapy, is predominantly mediated by triggering apoptosis in cancer cells^[47]. Recent studies have indicated that ISL induces prostate cancer cell apoptosis by disrupting mitochondrial function and activating caspase cascade signals^[14]. However, the role of ROS is not considered. The results of this study show that ISL increased intracellular ROS levels, and that ISL is capable of inducing HeLa cell apoptosis by reducing MMP. In addition, the levels of 89 kD fragment (active form) of PARP significantly increases, which is associated with the activation of caspase-3 and caspase-9; all these effects of ISL are antagonized by NAC.

The ER is the primary intracellular organelle responsible for protein folding, maturation, and trafficking^[48-49]. Unfolded or misfolded proteins accumulate in the ER lumen when the ER homeostasis is disturbed, resulting in ER stress. The three ER transmembrane proteins PERK, inositol-requiring protein-1 (IRE1a), and activating transcription factor-6 sense ER stress and induce specialized responses to recover or maintain ER function^[48]. Activated PERK phosphorylates the α -subunit of eukaryotic initiation factor-2 (eIF2) and eventually leads to the general inhibition of translation, thereby reducing the load of newly synthesized proteins that are translocated to the ER. Activated IRE1a splices X-box binding protein 1 (XBP1) mRNA. The XBP1 protein encoded by the spliced XBP1 mRNA enhances the capacity of the ER by upregulating the expression of ER chaperon proteins, such as the 78 kD glucose-regulated protein (GRP78), and reduces unfolded or misfolded proteins in the ER via the ER-associated protein degradation system (ERAD). ERAD regulates the degradation of unfolded or misfolded proteins in the ER through the ubiquitin (Ub)-proteasome system. However, if these protective responses fail and ER stress persists, specialized apoptotic pathways are activated to eliminate the damaged cells. ER stress-dependent apoptotic cell death is caused by the activation of ER-specific caspase-12^[50]. In the present study, we used the phosphorylation of PERK and eIF2 α as markers for ER stress, the expression of GRP78 as a marker for the protective ER stress response, and the expression of caspase-12 (full length) as a marker for the apoptotic ER stress response, in ISL-triggered HeLa cells apoptosis. As showed in Figure 5, the expression of p-PERK, p-eIF2 α , ER-related chaperones GPR78, and caspase-12 degradation were significantly increased

after exposure to ISL for 24 h. These effects are antagonized by cotreatment with NAC. Also, these results indicate that increased ER stress is involved, at least partially, in the ISL-triggered apoptosis of HeLa cells.

In conclusion, ISL induces oxidative stress in HeLa cells. The evidence demonstrates that ISL triggers oxidative stress to induce HeLa cell apoptosis through mitochondrial dysfunction, leading to the cleavage of PARP and activation of the caspase cascade-mediated signaling pathway. ISL also induces the expression of ER stress-related markers (GRP78), which subsequently trigger caspase-12 cleavage, resulting in apoptosis. Our evidence also demonstrates that ISL-induced apoptosis is implicated in ROS production. Moreover, extensive but fragmentary studies have shown that (i) ISL induces apoptosis in cancer cells^[13-15,17]; (ii) ISL induces excessive ROS generation in focal cerebral ischemia^[51]; and (iii) ISL induces apoptosis by disrupting mitochondrial function and activating caspase cascade signals in several cell types^[14]. However, ISL triggers oxidative stress to induce apoptosis through mitochondrial dysfunction in HeLa cells. Besides, ISL induces the expression of ER stress-related markers (GRP78) that subsequently trigger caspase-12 cleavage, resulting in apoptosis. A combination of these results provide more complete information on a better understanding of cancer prevention by using natural products. Evidence based on the aforementioned observations suggests that ISL has an important chemopreventive effect on human cancer.

REFERENCES

1. Kape R, Parniske M, Brandt S, et al. Isoliquiritigenin a strong nod gene-and glyceollin resistance-inducing flavonoid from soybean root exudate. *Appl Environ Microb*, 1992; 58, 1705-10.
2. Cao Y, Wang Y, Ji C, et al. Determination of liquiritigenin and isoliquiritigenin in *Glycyrrhiza uralensis* and its medicinal preparations by capillary electrophoresis with electrochemical detection. *J Chromatogr A*, 2004; 1042, 203-9.
3. Haraguchi H, Ishikawa H, Mizutani K, et al. Antioxidative and superoxide scavenging activities of retrochalcones in *Glycyrrhiza inflata*. *Bioorg Med Chem*, 1998; 6, 339-47.
4. Chin YW, Jung HA, Liu Y, et al. Anti-oxidant constituents of the roots and stolons of licorice (*Glycyrrhiza glabra*). *J Agric Food Chem*, 2007; 55, 4691-7.
5. Kim JY, Park SJ, Yun KJ, et al. Isoliquiritigenin isolated from the roots of *Glycyrrhiza uralensis* inhibits LPS-induced iNOS and COX-2 expression via the attenuation of NF-kappaB in RAW 264.7 macrophages. *Eur J Pharmacol*, 2008; 584, 175-84.
6. Tamir S, Eizenberg M, Somjen D, et al. Estrogen-like activity of glabrene and other constituents isolated from licorice root. *J Steroid Biochem Mol Biol*, 2001; 78, 291-8.
7. Yamamoto S, Aizu E, Jiang H, et al. The potent anti-tumor-promoting agent isoliquiritigenin. *Carcinogenesis*, 1991; 2, 317-23.
8. Baba M, Asano R, Takigami I, et al. Studies on cancer chemoprevention by traditional folk medicines, XXV. Inhibitory effect of isoliquiritigenin on azoxymethane-induced murine colon aberrant crypt focus formation and carcinogenesis. *Biol Pharm Bull*, 2002; 25, 247-50.
9. Lee CK, Son SH, Park KK, et al. Isoliquiritigenin inhibits tumor growth and protects the kidney and liver against chemotherapy-induced toxicity in a mouse xenograft model of colon carcinoma. *J Pharmacol Sci*, 2008; 106, 444-51.
10. li T, Satomi Y, Katoh D, et al. Induction of cell cycle arrest and p21(CIP1/WAF1) expression in human lung cancer cells by isoliquiritigenin. *Cancer Lett*, 2004; 207, 27-35.
11. Ma J, Fu NY, Pang DB, et al. Apoptosis induced by isoliquiritigenin in human gastric cancer MGC-803 cells. *Planta Med*, 2001; 67, 754-7.
12. Hsu YL, Kuo PL, Lin CC. Isoliquiritigenin induces apoptosis and cell cycle arrest through p53-dependent pathway in Hep G2 cells. *Life Sci*, 2005, 77, 279-92.
13. Jung JI, Chung E, Seon MR, et al. Isoliquiritigenin (ISL) inhibits ErbB3 signaling in prostate cancer cells. *Biofactors*, 2006; 28, 159-68.
14. Jung JI, Lim SS, Choi HJ, et al. Isoliquiritigenin induces apoptosis by depolarizing mitochondrial membranes in prostate cancer cells. *J Nutr Biochem*, 2006; 17, 689-96.
15. Takahashi T, Baba M, Nishino H, et al. Cyclooxygenase-2 plays a suppressive role for induction of apoptosis in isoliquiritigenin-treated mouse colon cancer cells. *Cancer Lett*, 2006; 231, 319-25.
16. Yoshida T, Horinaka M, Takara M, et al. Combination of isoliquiritigenin and tumor necrosis factor-related apoptosis-inducing ligand induces apoptosis in colon cancer HT29 cells. *Environ Health Prev Med*, 2008; 13, 281-7.
17. Auyeung KK, Ko JK. Novel herbal flavonoids promote apoptosis but differentially induce cell cycle arrest in human colon cancer cell. *Invest New Drugs*, 2010; 28, 1-13.
18. Iwashita K, Kobori M, Yamaki K, et al. Flavonoids inhibit cell growth and induce apoptosis in B16 melanoma 4A5 cells. *Biosci Biotechnol Biochem*, 2000; 64, 1813-20.
19. Schröder M, Kaufman RJ. ER stress and the unfolded protein response. *Mutat Res*, 2005; 569, 29-63.
20. Sitia R, Braakman I. Quality control in the endoplasmic reticulum protein factory. *Nature*, 2003; 426, 891-4.
21. Mori K. Tripartite management of unfolded proteins in the endoplasmic reticulum. *Cell*, 2000; 101, 451-4.
22. Biagioli M, Pifferi S, Raghianti M, et al. Endoplasmic reticulum

- stress and alteration in calcium homeostasis are involved in cadmium-induced apoptosis. *Cell Calcium*, 2008; 43, 184-95.
23. Kubota K, Lee DH, Tsuchiya M, et al. Fluoride induces endoplasmic reticulum stress in ameloblasts responsible for dental enamel formation. *J Biol Chem*, 2005; 280, 23194-202.
 24. Hung JY, Hsu YL, Ni WC, et al. Oxidative and endoplasmic reticulum stress signaling are involved in dehydrocostuslactone-mediated apoptosis in human non-small cell lung cancer cells. *Lung Cancer*, 2010; 68, 355-65.
 25. Malhotra JD, Miao H, Zhang K, et al. Antioxidants reduce endoplasmic reticulum stress and improve protein secretion. *Proc Natl Acad Sci U S A*, 2008; 105, 18525-30.
 26. Crack PJ, Taylor JM. Reactive oxygen species and the modulation of stroke. *Free Radic Biol Med*, 2005; 38, 1433-44.
 27. Klamt F, Dal-Pizzol F, Conte da Frota ML Jr, et al. Imbalance of antioxidant defense in mice lacking cellular prion protein. *Free Radic Biol Med*, 2001; 30, 1137-44.
 28. Ermak G, Davies KJ. Calcium and oxidative stress: from cell signaling to cell death. *Mol Immunol*, 2002; 38, 713-21.
 29. Shankar S, Srivastava RK. Involvement of Bcl-2 family members, phosphatidylinositol 3 ϕ -kinase/AKT and mitochondrial p53 in curcumin (diferulolylmethane)-induced apoptosis in Prostate Cancer. *Inter J Oncol*, 2007; 30, 905-18.
 30. Azam S, Hadi N, Khan NU, et al. Prooxidant property of green tea polyphenols epicatechin and epigallocatechin-3-gallate: implications for anticancer properties. *Toxicol In Vitro*, 2004; 18, 555-61.
 31. Fujisawa S, Kadoma Y. Anti- and pro-oxidant effects of oxidized quercetin, curcumin or curcumin-related compounds with thiols or ascorbate as measured by the induction period method. *In Vivo*, 2006; 20, 39-44.
 32. Takahashi T, Takasuka N, Iigo M, et al. Isoliquiritigenin, a flavonoid from licorice, reduces prostaglandin E2 and nitric oxide, causes apoptosis, and suppresses aberrant crypt foci development. *Cancer Sci*, 2004; 95, 448-53.
 33. Lee YM, Lim do Y, Choi HJ, et al. Induction of cell cycle arrest in prostate cancer cells by the dietary compound isoliquiritigenin. *J Med Food*, 2009; 12, 8-14.
 34. Mosmann T. Rapid colorimetric assay for cellular growth and survival: application to proliferation and cytotoxicity assays. *J Immunol Methods*, 1983; 65, 55-63.
 35. Wang C, Eshleman J, Lutterbaugh J, et al. Spontaneous apoptosis in human colon tumor cell lines and the relation of wt p53 to apoptosis. *Chin Med J (Engl)*, 1996; 109, 537-41.
 36. Vanden Hoek TL, Li C, Shao Z, et al. Significant levels of oxidants are generated by isolated cardiomyocytes during ischemia prior to reperfusion. *J Mol Cell Cardiol*, 1997; 29, 2571-83.
 37. Cechetti F, Fochesatto C, Scopel D, et al. Effect of a neuroprotective exercise protocol on oxidative state and BDNF levels in the rat hippocampus. *Brain Res*, 2008; 1188, 182-8.
 38. Bradford MM. A Rapid and Sensitive Method for the Quantitation of Microgram Quantities of Protein Utilizing the Principle of Protein-Dye Binding. *Anal Biochem*, 1976; 72, 248-54.
 39. Hockenbery D, Nunez G, Millman C, et al. Bcl-2 is an inner mitochondrial membrane protein that blocks programmed cell death. *Nature*, 1990; 348, 334-46.
 40. Reers M, Smith TW, Chen LB. J-Aggregate formation of a carbocyanine as a quantitative fluorescent indicator of membrane potential. *Biochemistry*, 1991; 30, 4480-6.
 41. Smiley ST, Reers M, Mottola-Hartshorn C, et al. Intracellular heterogeneity in mitochondrial membrane potentials revealed by a J-aggregate-forming lipophilic cation JC-1. *Proc Natl Acad Sci USA*, 1991; 88, 3671-5.
 42. Hanahan D, Weinberg RA. Weinberg. Hallmarks of Cancer: The Next Generation. *Cell*, 2011; 44, 646-74.
 43. Hengartner MO. The biochemistry of apoptosis. *Nature*, 2000; 407, 770-6.
 44. Brown JM, Wouters BG. Apoptosis, p53, and tumor cell sensitivity to anticancer agents. *Cancer Res*, 1999; 59, 1391-9.
 45. Rottner M, Tual-Chalot S, Mostefai HA, et al. Increased oxidative stress induces apoptosis in human cystic fibrosis cells. *PLoS One*, 2011; 6, e24880.
 46. Kaneto H, Kawamori D, Matsuoka TA, et al. Oxidative stress and pancreatic beta-cell dysfunction. *Am J Ther*, 2005; 12, 529-33.
 47. Marfe G, Di Stefano C. *In vitro* anti-leukaemia activity of pyrrolo[1,2-b][1,2,5]benzothiadiazepines (PBTDS). *Recent Pat Anticancer Drug Discov*, 2010; 5, 58-68.
 48. Ron D, Walter P. Signal integration in the endoplasmic reticulum unfolded protein response. *Nat Rev Mol Cell Biol*, 2007; 8, 519-29.
 49. Todd DJ, Lee AH, Glimcher LH. The endoplasmic reticulum stress response in immunity and autoimmunity. *Nat Rev Immunol*, 2008; 8, 663-74.
 50. Nakagawa T, Zhu H, Morishima N, et al. Caspase-12 mediates endoplasmic-reticulum-specific apoptosis and cytotoxicity by amyloid- β . *Nature*, 2000; 403, 98-103.
 51. Zhan C, Yang J. Protective effects of isoliquiritigenin in transient middle cerebral artery occlusion-induced focal cerebral ischemia in rats. *Pharmacol Res*, 2006; 53, 303-9.